Scientific Research Publishing

International Journal of Geosciences, 2025, 16(1), 1-19
https://www.scirp.org/journal/ijg
ISSN Online: 2156-8367
ISSN Print: 2156-8359

Preliminary Report on the Paleoproterozoic Metasediments Genesis and Features of the Banfora Belt Western Burkina Faso (West Africa Craton)

Hermann Ilboudo[1*], Bernadin Gnamou[1], Wilfried Antoine Bassou Toe[1], Marc Ephrem Allialy[2]

[1]Laboratoire Géosciences et Environnement, Département des Sciences de la Terre, Université Joseph KI-ZERBO, Ouaga, Burkina Faso
[2]Laboratoire de Géologie du Socle et de Métallogénie, UFR STRM, Université Félix Houphouët-Boigny de Cocody Abidjan, Abidjan, Côte d'Ivoire
Email: *hermann.ilboudo@ujkz.bf

How to cite this paper: Ilboudo, H., Gnamou, B., Toe, W.A.B. and Allialy, M.E. (2025) Preliminary Report on the Paleoproterozoic Metasediments Genesis and Features of the Banfora Belt Western Burkina Faso (West Africa Craton). *International Journal of Geosciences*, **16**, 1-19.
https://doi.org/10.4236/ijg.2025.161001

Received: November 7, 2024
Accepted: January 4, 2025
Published: January 7, 2025

Abstract

Metasedimentary rocks of the Banfora belt are examined for their petrography geochemistry and genesis. The main formations are pelite metapelites sandstone, and metagraywackes. The first ones show a fine interlocking layering with unclear graded bedding in the sandstone compared to the metapelites, while the metagraywackes show a clearly discordant graded bedding of light grey to light pink color. The low SiO_2/Al_2O_3 ratios (3.67 to 6.60) suggest their low sedimentary maturity. The metapelites and sandstone-pelites show moderate Na_2O/K_2O values (10.13 - 22.69), indicating moderate chemical maturity; in contrast, the metagraywackes show low Na_2O/K_2O values (1.94 - 5.80) suggesting low chemical maturity. The metapelites, sandstone-pelites and metagraywackes have Rb/Sr ratios of 0.866 - 0.004 and 0.173 - 0.607 respectively, indicating a moderate to low degree of chemical alteration. The chemical alteration index (CIA = 58 - 83) and the plagioclase alteration index (PIA = 53 - 81) suggest weak to moderate alteration of the source rocks. This alteration is different from simple alteration as the sole control of chemical composition, but is associated with metasomatism. The metapelites sandstone shows a mixture of mafic and intermediate igneous sources, which indicates that the protoliths could be basalts and andesites, but the metagraywackes would be derived from the erosion of a mixture of andesitic to granitic rocks. The studied rocks were generated from young undifferentiated to differentiated arcs. They are of low to moderate sedimentary and chemical maturity.

Keywords

Metasediments, Banfora Belt, Source, Alteration, Geotectonic Environment

1. Introduction

The geochemical composition of sedimentary rocks records their sources and tectonic history [1]-[7]. During meteoric weathering of rocks, alkali and alkaline-earth elements with high solubility in meteoric waters have greater fractionation potential; thus, their concentration in fine-grained sedimentary rocks may not be representative of their origin. On the other hand, rare earth elements, yttrium, scandium and thorium, with low solubility in water, can provide information about their sources [3] [5] [6] [8]. In addition, sedimentary deposition can occur in a wide range of environments within evolving accretionary and collisional orogenic systems, from marginal basins in volcanic arcs to forearc and back-arc basins in collisional orogens [9] [10]. The types of supracrustal successions that develop within these systems can exhibit significant variability in terms of their geometry, stratigraphy, sediment provenance and structural event [10]. The Birimian Belts are characterized by a lithostratigraphy comprising tholeiitic to lower calc-alkaline basaltic suite with some intercalations of sedimentary rocks, overlain by a thick detrital series with carbonate intercalations in association with calc-alkaline plutonic and volcanic rocks [11]-[19]. However, sedimentation in the West African Craton (WAC) was diachronous during the Eburnean orogeny [10] [20]. This is also reflected in the lithostratigraphy, with shallow water deposits to the east of the WAC, while carbonates are only present in the younger successions to the west [10]. The deposits of the volcano sedimentary sequence occurred over more or less extended periods of time and can be grouped into deep water and shallow water series [10]. The shallow water series were deposited mainly on older volcanic series [10] [21] [22]. The deep-water sequences (2160 - 2065 Ma) were defined within a longer depositional interval than the shallow-water series (2160 - 2115 Ma), although both were deposited simultaneously during the later stages of regional sedimentation [10]. The present study deals with preliminary petrographic and geochemical data from the metasediments of the Banfora belt, which extends into Côte d'Ivoire as the Katiola Marabadiassa belt and the Bandama volcano-sedimentary basin [11] [15] [23] [24]. The Banfora belt appears to be poorly documented compared to the other western belts in Burkina (Houndé and Boromo) in terms of the nature of their sedimentary deposits [13] [25] [26]. Recent syntheses suggest that the sedimentary deposits of Banfora, Boromo and the western part of Houndé occurred in deep water over a long period that is supported by contemporary volcanic activity [10]. Unlike the Banfora and Boromo belts, the Houndé belt contains Tarkwaïan-type sediment units [13] [26] [27]. In the southern part of the Banfora belt, Pb-Pb zircon ages have been found in detrital sediments from the Bandama basin in Côte d'Ivoire, including detrital zircons dated between 2133 and 2107 ± 7 Ma, so the age of sediment deposition is estimated between 2108 ± 12 and 2097 ± 3 Ma [24]. Although some authors have shown the depositional environment of sediments in the Boromo and Houndé belts, that of the Banfora belt remains unknown. In this study, we will discuss the petrographic and geochemical characteristics of the sedimentary rocks in this part of the Birimian system.

2. Geological Setting

Various studies [22] [27]-[31] present the geological configuration of the Léo/Man shield in two domains (**Figure 1**), respectively the western Kénéma-Man domain > 2500 Ma and the eastern Baoulé-Mossi domain dated at 2000 Ma [28] [32]. The Baoulé-Mossi domain consists mainly of volcanic and sedimentary belts and granitoid intrusions [10] [12] [13] [22] [27] [33]-[37]. Burkina Faso, which extends over the Baoulé-Mossi domain, is composed of a Paleoproterozoic basement of greenstone and granitoid belts (80%) covered on its western, northern and eastern margins by Neoproterozoic to Cambro-Ordovician sedimentary formations (1000 - 435 Ma) (20%). The belts are essentially made up of metavolcanic rocks, ranging from meta basalts to meta rhyolites and metasedimentary rocks including quartzites and metapelites [13] [14] [38] [39]. More specifically, the Banfora belt, which is 160 km long and 35 km wide [14] in Burkina Faso, extends as far as Côte d'Ivoire and is intersected by the Greenville-Ferkéssédougou-Bobo-Dioulasso major shear zone (**Figure 2**). The eastern part of the Banfora belt is made up of interbedded units of basalts, andesites, volcano sediments and

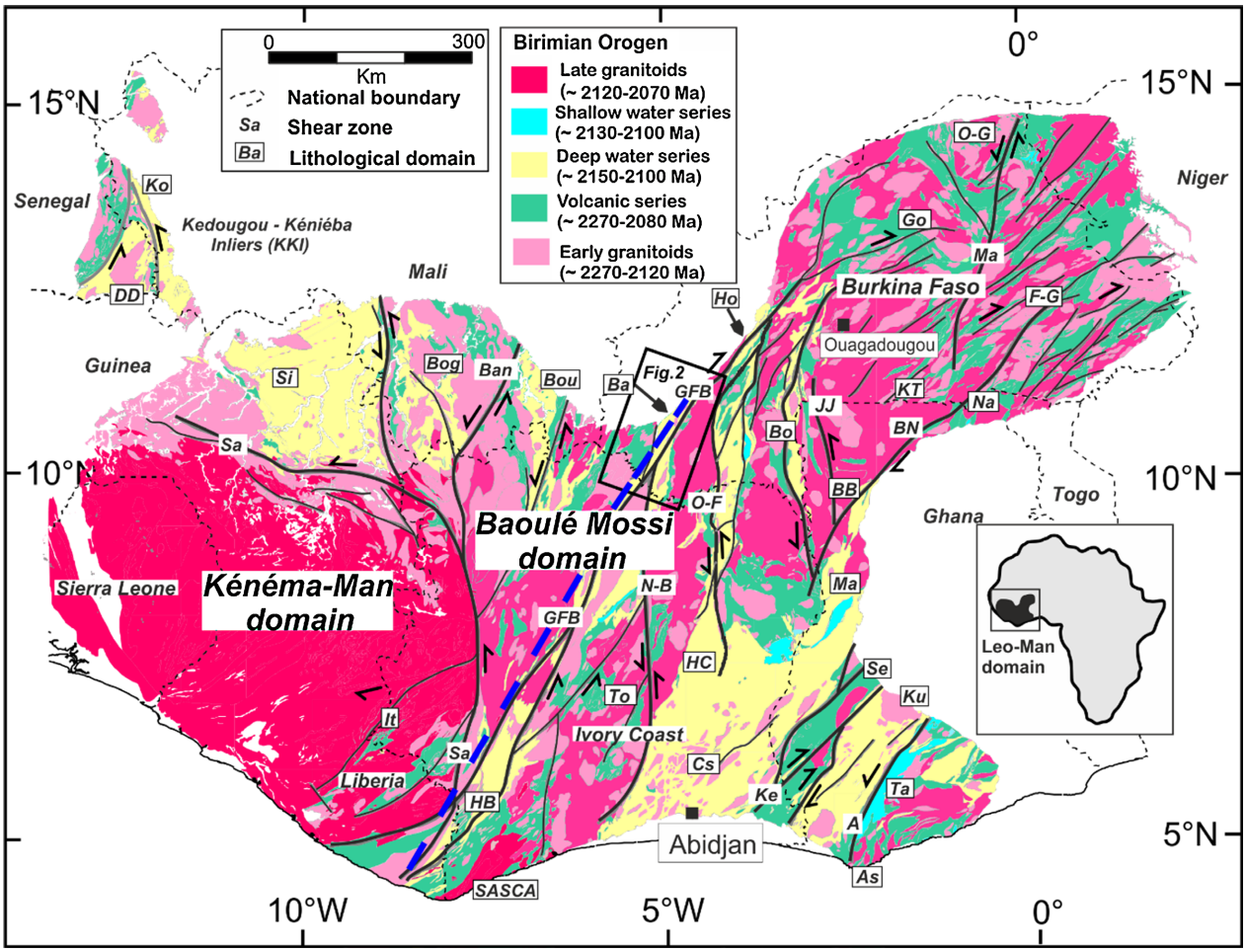

Figure 1. Geological map of the Leo/Man shield and the most important gold deposits across the WAC (modified from Grenholm *et al.* 2019).

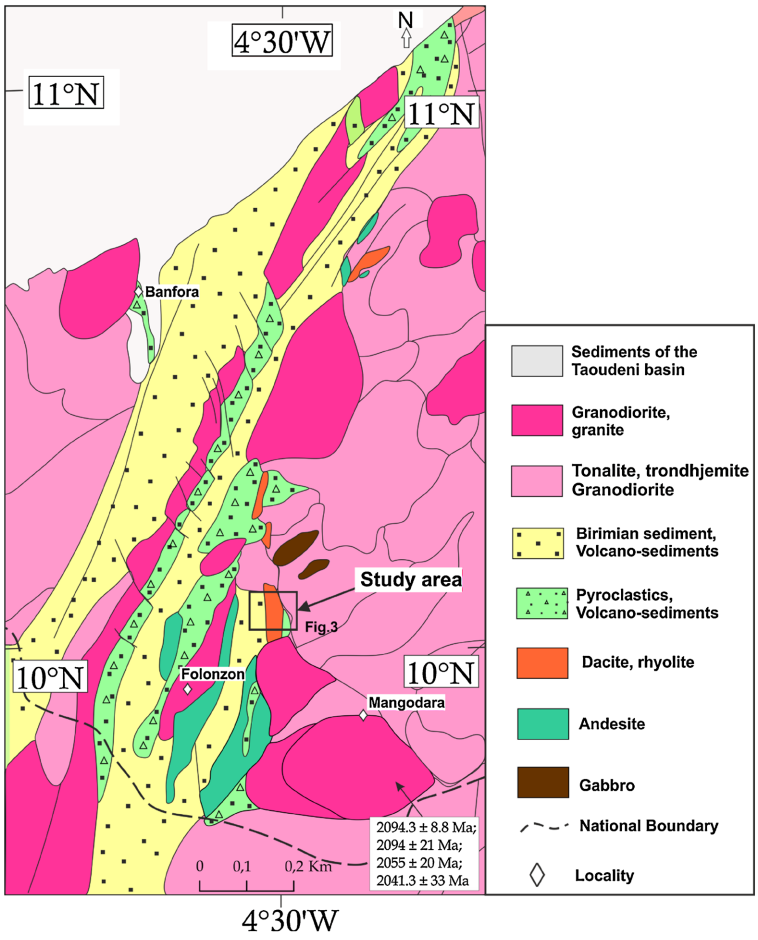

Figure 2. Simplified geological map of Banfora green belt (modified from Metelka *et al.*, 2011) and location of the studied area.

rhyolites, 2 to 4 km thick, while the western part is composed solely of volcano sediments [13]. The overall stratigraphy of the belt, as proposed by [13] and revised by [14], suggests, from bottom to top: 1) deposition of ultramafic rocks, 2) deposition of mafic volcanics, 3) subsequent deposition of lava flows and projections (pyroclastites and lapilli tuff), 4) deposition of siliceous rocks (exhalite), 5) deposition of pelitic and turbiditic sediments, 6) deposition of the pre-collisional eastern granite and 7) deposition of the post-collisional western granite. The volcanic activity that prevailed in western Burkina Faso took place between 2190 Ma and 2160 Ma (Eburnean), according to [13] and has a juvenile character with respect to εHf (0 to + 8) [40]. Exhalites constitute the upper horizon of the lithostratigraphy of volcanic formations in the eastern part of the belt, while subvolcanic rocks are mainly porphyritic micro diorite, sills and dolerite dykes [14].

Syn-tectonic intrusions (granite and granodiorite) emplaced by the Greenville-Ferkéssédougou-Bobo-Dioulasso regional shear zone known from Liberia and Côte d'Ivoire [13] [14] [41]. Based on the geochemical and geotectonic framework, [14] pointed out that the granitoids of the western and eastern margins of the Banfora belt are post- and pre-collisional, respectively. Geochemically, the

granitoid intrusions are arc volcanic in nature, including negative Ta, Nb and Sr anomalies and mostly older than 2100 Ma [40]. In the neighboring area, the pegmatite associated with granitoids and migmatitic gneiss potentially contains rare metals [37] [42]. More specifically, the geology of the study area consists of a series of mainly metamorphosed volcanic formations (rhyolite, rhyolitic tuff, dacite, andesite, basalt, etc.). Rare outcrops of highly siliceous sulphidic felsic formations (rhyolite, cherts and quartzites) that have resisted alteration appear to be the main host rocks [39]. Late monzonite, granodiorite and diorite crosscut the volcanic assemblage.

3. Methodology

3.1. Sampling

The fieldwork consisted of outcrop description and diamond drill core logging, followed by sampling. Core samples were taken from two drill cores (K01 and K02), to ensure good spatial coverage of the study areas. In all, around ten rock samples from these boreholes were collected. Sampling was carried out on different facies. A dozen thin sections were taken at the Geosciences and Environment Laboratory (LaGE) at Joseph KIZERBO University. The detailed investigation was carried out under a Nikon Eclipse 50i POL polarizing microscope coupled to a camera. We use acronyms for rock-forming minerals in [43].

3.2. Analytical Method

Part of this study is based on whole-rock geochemical data from drill cores. Samples were analyzed by XRF diffraction for major elements, rare earth, and trace elements using inductively coupled plasma mass spectrometry (ICPMS) at the ACME laboratory in Vancouver. Twenty-one of the analyzed samples comprise andesite, dacite and rhyolite (**Table 1**). The samples were crushed and pulverized at 200 mesh, and sample fragments (0.2 g) were placed in graphite crucibles with the addition of lithium borate flux. The crucibles were placed in an oven and heated to 1025˚C for 25 min. Each molten sample was then dissolved in 5% HNO_3. A blank and an internal standard (STD SO15 reference material) were weighed, digested and analyzed for accuracy. Calibration standards, verification standards and reagent blanks were also added to the sample sequence for testing.

4. Results

4.1. Lithology

4.1.1. Meta Pelitic Sandstone-Facies

The metapelites sandstone-pelitic facies are made up of metapelites, metasandstone and meta arkoses. The metapelites form an ill-defined contact with black cherts, but are easily identified by their alternation of dark and light beds (**Figure 3(a)**). They form the top of the lithostratigraphic sequence. These rocks are alternating black and whitish, giving a ribbon-like structure. They are locally characterized by millimeter to centimeter-high beds alternating with fine beds of black

Table 1. Litho geochemical data of the metasedimentary rocks of the Banfora belt.

Sample Name Lithology	K01 Meta pelite sandstone	K01 Meta Sandstone-pelite	K02 Metagrauwackes	K02 Meta grauwackes	K02 Meta grauwackes	K02 Meta grauwackes
SiO_2	62.281	41.366	73.967	71.742	70.587	79.229
Al_2O_3	16.945	10.751	11.294	12.564	12.681	11.991
Fe_2O_3	12.994	41.182	4.533	5.062	5.405	2.717
CaO	0.925	1.321	2.626	1.368	0.336	0.764
MgO	0.605	0.781	0.912	0.837	0.288	0.768
Na_2O	0.065	0.140	0.896	0.562	0.826	0.690
K_2O	1.466	1.420	1.742	3.261	2.902	2.335
TiO_2	0.756	0.491	0.372	0.556	0.166	0.134
P_2O_5	0.243	0.066	0.948	0.584	0.552	0.479
MnO	0.190	0.056	0.040	0.020	0.010	0.030
LOI	2.127	0.641	1.200	2.320	5.121	0.230
Total	98.596	98.215	98.531	98.877	98.875	99.367
Trace						
Ag	0.122	0.406	0.250	1.600	0.250	0.250
As	9.656	18.266	47.300	89.700	4053.700	123.900
Ba	1167.866	625.304	716.100	700.800	605.100	685.800
Be	0.818	0.315	0.890	0.550	0.510	0.860
Bi	0.109	0.054	0.070	0.150	0.200	0.020
Cd	0.096	0.102	0.130	0.060	0.390	0.060
Co	24.979	19.020	9.200	6.600	34.200	5.600
Cr	158.922	112.698	36.000	128.000	143.000	20.000
Cs	1.407	2.127	4.310	9.880	3.500	2.710
Cu	44.049	16.188	5.000	23.000	57.000	8.000
Hf	4.239	3.126	2.040	3.130	3.370	2.200
Li	12.176	38.622	14.400	30.900	25.900	28.200
Mn	1.471	0.333	334.000	204.000	98.000	225.000
Mo	1.640	78.567	0.500	2.500	3.900	1.100
Nb	10.320	6.359	4.420	5.370	1.320	3.010
Ni	48.563	61.902	11.000	3.000	89.000	7.000
Pb	4.612	3.749	11.600	32.800	22.300	10.100
Rb	46.888	32.059	52.800	89.330	77.290	64.190
Sb	2.325	5.497	3.340	8.700	18.190	2.260

Continued

Sc	30.911	19.444	7.300	15.200	20.000	4.200
Sr	54.105	74.920	305.070	230.190	127.270	163.820
Ta	0.754	0.461	0.450	0.440	0.180	0.340
Th	5.444	3.245	5.290	4.420	4.040	6.450
Ti	4.573	3.054	0.223	0.333	0.100	0.080
U	2.107	1.303	1.100	1.290	1.620	1.430
V	188.224	244.641	76.000	115.000	113.000	40.000
W	0.757	0.797	0.700	3.600	0.900	1.600
Y	17.628	16.539	10.980	12.330	7.180	8.960
Zn	152.255	210.596	39.000	21.000	58.000	36.000
Zr	162.213	113.204	77.000	128.200	125.200	71.900
REE						
La	26.069	19.863	25.960	25.890	19.730	25.170
Ce	54.291	41.346	53.630	55.200	42.380	49.890
Pr	5.938	4.740	6.241	6.658	4.886	5.578
Nd	20.877	16.806	22.650	24.610	18.040	19.460
Sm	3.820	2.596	3.980	4.580	3.300	3.200
Eu	1.167	0.893	1.050	1.160	0.760	0.840
Gd	3.356	2.460	3.020	3.190	2.420	2.350
Tb	0.514	0.424	0.397	0.405	0.329	0.326
Dy	3.191	2.757	2.290	2.280	1.750	1.760
Ho	0.701	0.613	0.450	0.470	0.310	0.350
Er	2.037	1.721	1.220	1.410	0.860	0.970
Tm	0.314	0.255	0.180	0.220	0.140	0.140
Yb	2.089	1.591	1.070	1.480	0.890	0.930
Lu	0.346	0.255	0.161	0.228	0.146	0.138
Th/U	2.585	2.490	4.809	3.426	2.494	4.510
SiO_2/Al_2O_3	3.676	3.848	6.549	5.710	5.566	6.607
K_2O/Na_2O	22.697	10.135	1.944	5.801	3.512	3.384
Rb/Sr	0.867	0.428	0.173	0.388	0.607	0.392
Zr/Sc	5.248	5.822	10.548	8.434	6.260	17.119
Th/Sc	0.176	0.167	0.725	0.291	0.202	1.536

cherts. Their primary bedding is preserved and marked by alternating dark beds of glauconite-graphite and light beds of carbonate-biotite (Figure 3(b)). The carbonate-biotite beds are in close contact with the glauconite beds and vary in thickness from 5 mm to 1 cm. Quartz can represent up to 90% to 95% of the quartz-biotite beds, which are also in close contact with the glauconite beds. In places,

this unit consists of folded graphitic beds one centimeter thick, which appear as a turbidite sequence.

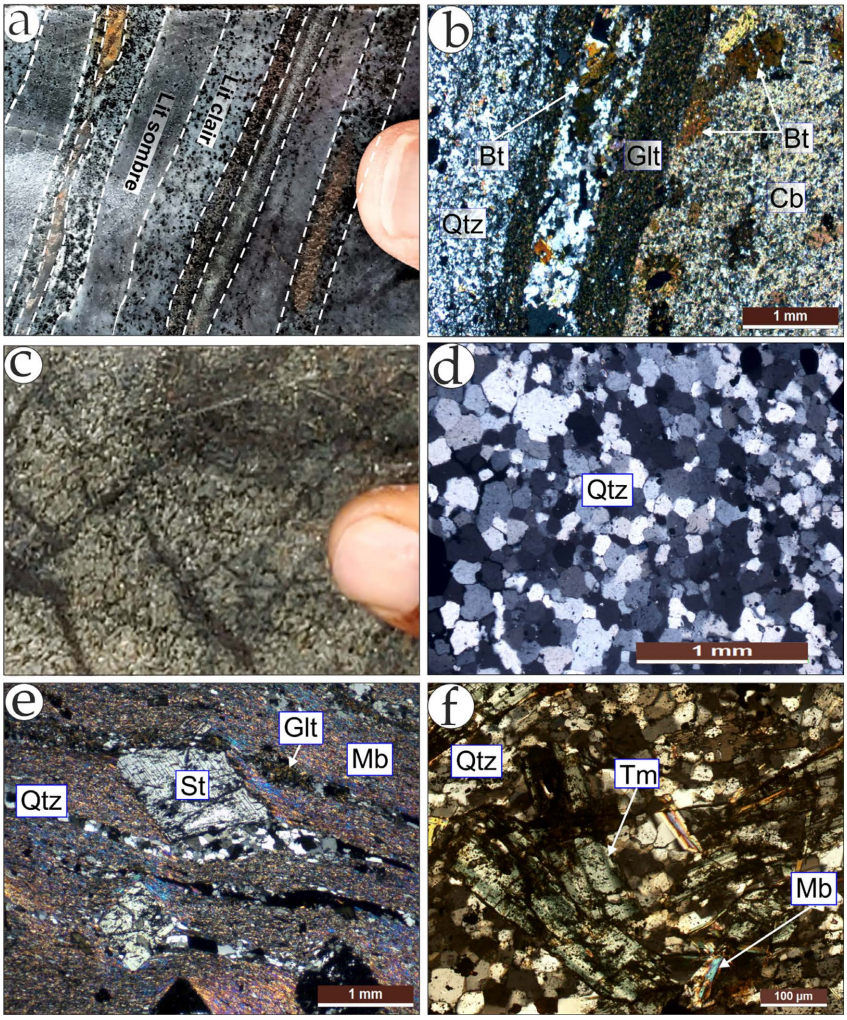

Figure 3. Samples from drill core and microphotograph of the main lithologies. (a): Banded metapelite; (b): Metapelite with alternating quartz—biotite, glauconite and carbonate—biotite; (c): Sandstone; (d): Heterogranular quartz in sandstone; (e): Alternating beds of quartz-glauconite and sericite in sandstone; (f): Tourmaline porphyroblast in sandstone. Qtz: Quartz; Bt: Biotite; Glt: Glauconite; Cb: Carbonate; Tm: Tourmaline; St: Staurolite.

The metasandstone has a fine, crisscrossed stratification (**Figure 3(c)**) with unclear graded bedding (**Figure 3(d)**). They consist of ±foliated, mylonitic texture formed by staurolite porphyroblasts (**Figure 3(e)**). The metasandstone in contact with the monzogranite shows tourmaline porphyroblasts (**Figure 3(f)**). Their mineralogy essentially consists of staurolite porphyroblasts, quartz beds (50%), white micas (25%), and glauconites (5%) parallel to subparallel in a quartz matrix, with tourmaline micro-clusters. The staurolite porphyroblasts are moulded into the white mica beds and dwell unaltered. Tourmaline porphyroblasts are in micro-clusters in a white quartz-mica matrix background and often show fine recrystallisation of phyllite of white micas and quartz inclusions.

4.1.2. Metagraywackes

The metagrauwackes are bedded and show clearly discordant light grey to light pink graded bedding (Figure 4(a)). The bedding is fine and coarse, composed of intergrown quartz in which some phyllite minerals of white micas and biotite, and cherts and felsic clasts are encrusted (Figure 4(b)). The cherty clasts are composed of quartz, while the felsic clasts, about 1 to 2 cm long, are sub-angular and contain small crystals of white micas and quartz. The metagraywackes are composed of breccias supported by angular clasts in a carbonatitic matrix. They appear to be variable, both in terms of grain shape and mineralogical composition. Mature minerals are composed of quartz grains (75%) with blunt contours and, secondarily, plagioclase (5%), while immature one is made up of angular to sub-angular quartz-feldspar grains (70%). The mineralogy is presented by fragments of quartz (0.5 mm) and albite (0.5 mm) of around 1% to 2% in quartz cement (50% to 60%) white mica (30% to 40%) in the mature deposits (Figure 4(c)), while the immature ones are made up of 30% to 35% quartz, 1% amphibole, 5% orthoclase, 10% biotite and 40% to 50% white micas (Figure 4(d)).

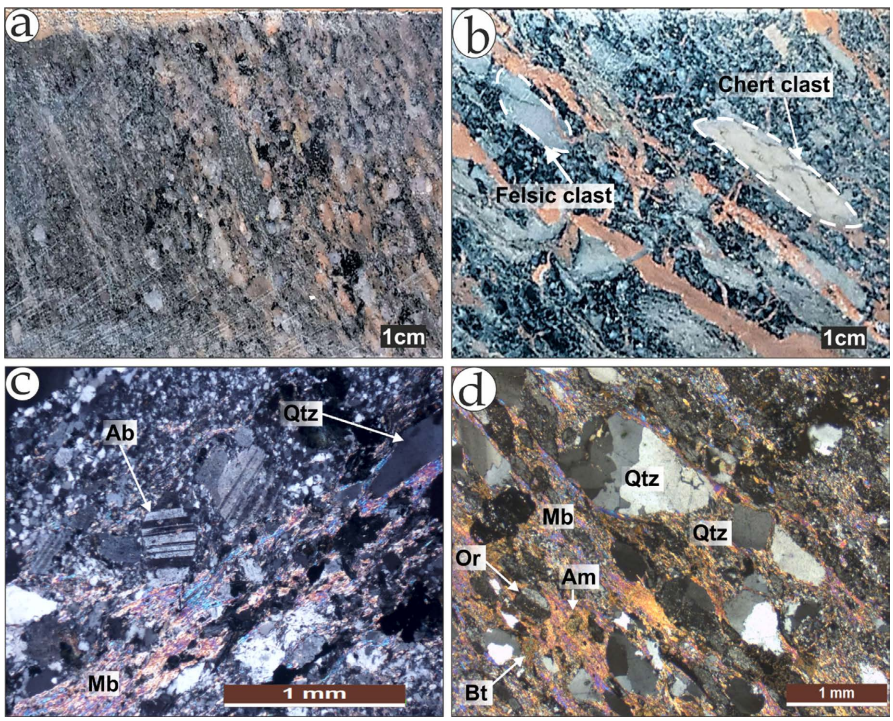

Figure 4. Samples from drill core and microphotograph of the main lithologies. (a): Grauwackes showing granoclassing; (b): metagraywackes with felsic clasts and chert clasts; (c): Feldspar-rich metagraywackes; (d): metagraywackes' rich in white mica.

4.2. Geochemical Data

4.2.1. Composition of Major Elements

In the metapelite sandstone, SiO_2 ranges between 41.04 and 62.28 wt%, and Al_2O_3 values range from 7.42 to 16.94 wt%. Majors such as MgO and CaO show high contents of 8.56 - 12.99 wt% and 0.92 - 29.94 wt% respectively, while K_2O and

Na_2O show low values of 0.008 - 1.466 and 0.001 - 0.064 wt% respectively. TiO_2 and Fe_2O_3 concentrations vary between 0.37 - 0.75 wt% and 0.6 - 1.55 wt% respectively.

The metagraywackes are more siliceous with (SiO_2 = 70.58 - 79.22 wt%. These samples show MgO = 0.28 - 0.91 wt% and CaO = 0.33 - 2.62 wt%) and moderate K_2O = 1.74 - 3.26 wt% and Na_2O = 0.562 - 0.896 wt%. TiO_2 and Fe_2O_3 contents ranged from 2.71 - 5.40 wt% and 0.13 - 0.55 wt% respectively.

The sedimentary rocks were classified using the log (Fe_2O_3/K_2O) versus log (SiO_2/Al_2O_3) binary diagram [44]. In this diagram, the metapelite sandstone belongs to the iron-rich sandstone group, while the metagraywackes belong to the wakes group, evolving towards the litharenites group (Figure 5).

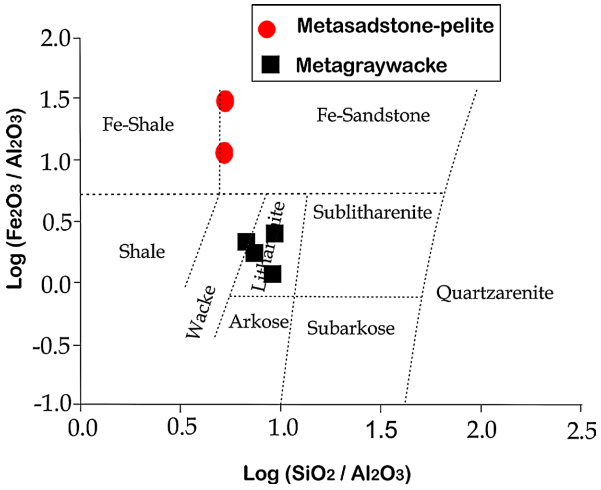

Figure 5. Classification of the studied metasedimentary rocks using log (Fe_2O_3/K_2O) versus log (SiO_2/Al_2O_3) (after Herron, 1988).

4.2.2. Trace Element Composition

The composition of high field strength trace elements (Nb, Ta, Zr, Hf, Sc, Y); large Ion lithophile elements (Rb, Sr, Ba, Cs, Cu, Pb, U, Th) and transition metals (Mn, Sc, V, Cr, Co, Ni, Cu, Zn) vary greatly in metasedimentary rocks (Table 1). The levels of Nb (1.32 - 5.36 ppm), Ta (0.18 - 0.44 ppm), Zr (71.9 - 128.19 ppm), Sc (4.19- 3.36 ppm), Rb (52.79 - 89.33 ppm), Sr (127.26 - 305.07 ppm) confirm this variability in the metagraywackes. Similarly, the metapelites sandstone show variable contents of Nb (6.35 - 10.32 ppm), Ta (0.46 - 0.75 ppm), Zr (113.20 - 128.19 ppm), Sc (19.44 - 30.19 ppm), Rb (22.05 - 46.88 ppm), Sr (54.10 - 74.92 ppm).

5. Discussion

5.1. Lithological Characteristics

The sedimentary units of the Banfora belt are essentially composed of metasandstone—pelitic and metagraywackes rocks. Metapelites sandstone and metagraywackes are the main component of the Birimian basins [7] [10] [45]-[49]. The metapelites rocks studied are mainly composed of glauconite and graphite, as-

suming that they were formed in a marine environment. In the metagraywackes facies, the sedimentological characteristics are more or less preserved through the fine- and coarse-grained bedding. The felsic volcanoclastite clasts observed in the metagraywacke indicate the initial emplacement of felsic volcanoclastite prior to the filling of the basin. They were deposited over an extended period of time that is supported by contemporary volcanic activity [10] [13] [17] [22] [24] [50]-[52]. The geochemistry of sedimentary rocks provides information on several factors: 1) sedimentary maturity indicated by the SiO_2/Al_2O_3 ratio which is a function of the proportion of quartz and clay minerals/feldspars and chemical maturity marked by the Na_2O/K_2O ratio which highlights the presence of feldspars [44]; and 2) the mineral stability index marked by the Fe_2O_3/K_2O ratio relating to the proportion of ferromagnesian minerals to plagioclases [53]. The low SiO_2/Al_2O_3 ratios (3.67 to 6.60) in the rocks suggest their low sedimentary maturity. The metapelites sandstone record moderate Na_2O/K_2O values (10.13 - 22.69), indicating moderate chemical maturity; on the other hand, the metagraywackes show low Na_2O/K_2O contents (1.94 - 5.80), suggesting low chemical maturity. In fact, the geochemical and isotopic data for Birimian sedimentary rocks suggest an immature nature with very little recycled material [7]. Moreover, compared with the upper continental crust (**Figure 6**), these Birimian rocks are depleted in alkaline and alkaline-earth elements and enriched in transition metals [7] [47].

5.2. Alteration and Diagenesis

Although petrographic data on the alteration of sedimentary rocks can be useful, no quantification studies have yet been carried out. Furthermore, diagenesis also commonly involves the alteration of feldspars and other unstable minerals to clay, so it can be difficult to determine these processes through the use of geochemical data [4] [54]. However, the Rb/Sr ratio and the chemical index of alteration (CIA) have been established as a general guide to the degree of alteration [4]. The metasandstone-pelites and metagraywackes have Rb/Sr ratios between 0.866 - 0.004 and 0.173 - 0.607 respectively, indicating a moderate to low degree of chemical alteration. In addition, the studied samples have ACNK values ranging from 58 - 83 and plagioclase alteration index (PIA) values from 53 - 81 respectively, suggesting weak to moderate alteration of the source of the rocks. In the ACNK diagram, the samples show more or less linear trends, but this is not comparable with simple alteration as the only control on chemical composition (**Figure 7**). This pattern indicates the contribution of K to the samples as a result of metasomatism.

5.3. Geotectonic Setting and Sources of Sedimentary Rocks

Several authors have used the chemical composition of sedimentary rocks to distinguish their geotectonic context [4] [55] and defined four types of sedimentary terrain: 1) ancient upper continental crust (UGC), 2) recycled sedimentary rocks (RSR), 3) undifferentiated young arc (YUA) and 4) differentiated young arc

(YDA). The Banfora sedimentary rocks compared to the upper continental crust show relatively low to moderate but variable values of SiO_2/Al_2O_3, K_2O/Na_2O and lower ratios of IAC and incompatible to compatible elements (Figure 8) such as Th/Sc (0.16 - 1.53) and Zr/Sc (5.24 - 17.11). These geochemical characteristics suggest that the metasandstone and metagraywackes originate from young undifferentiated to differentiated arcs.

The SiO_2 vs K_2O/Na_2O diagram of [55] shows that the meta sandstone-pelite samples formed in active continental margin and passive continental margin environments, whereas the metagraywackes formed in an active continental margin environment (Figure 9(a)). Furthermore, the Th vs Th/U diagram of [4] indicates

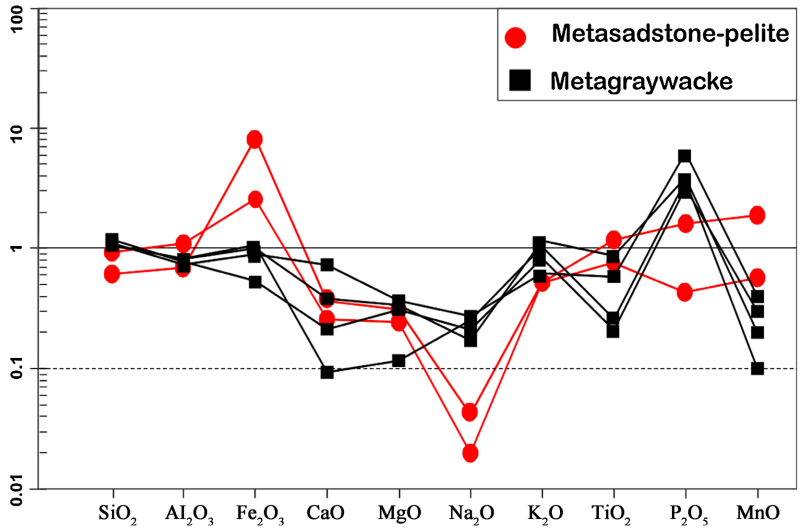

Figure 6. Upper continental crust normalized major element plots for the studied metasedimentary rocks. Upper continental crust values are from Rudnick and Gao (2014).

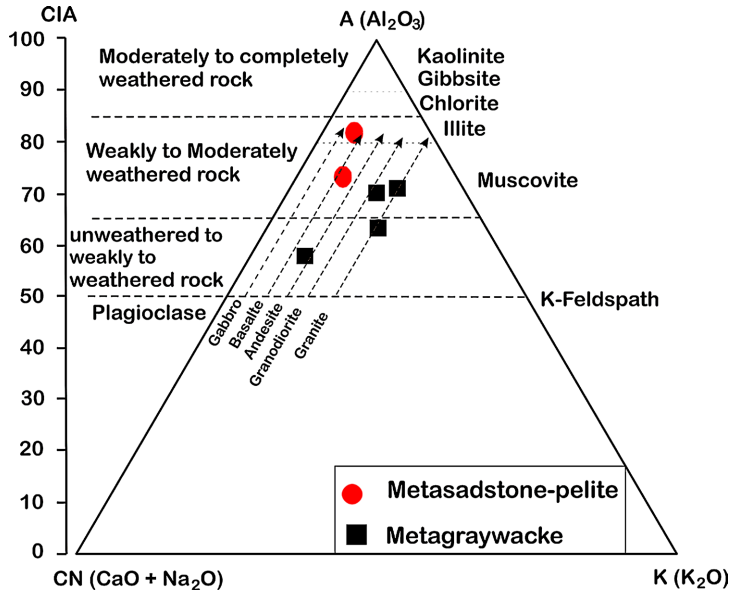

Figure 7. Al_2O_3-(CaO +Na_2O)-K_2O diagram for the metasedimentary rocks of the Banfora belt (after Nesbitt and Young, 1984).

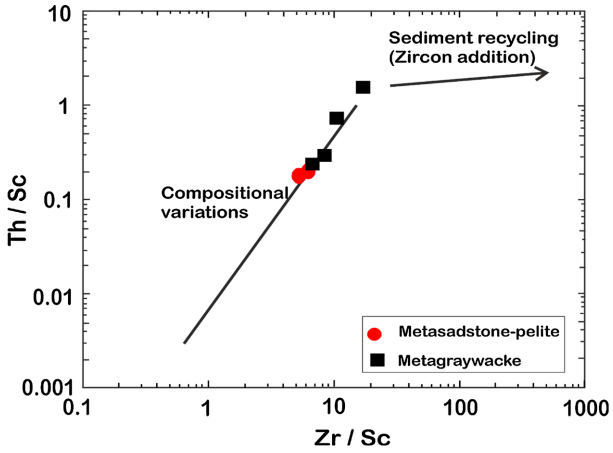

Figure 8. Plot of Th/Sc versus Zr/Sc for the metasedimentary rocks of the Banfora belt. The compositional variation trend lines are from McLennan *et al.* (1993).

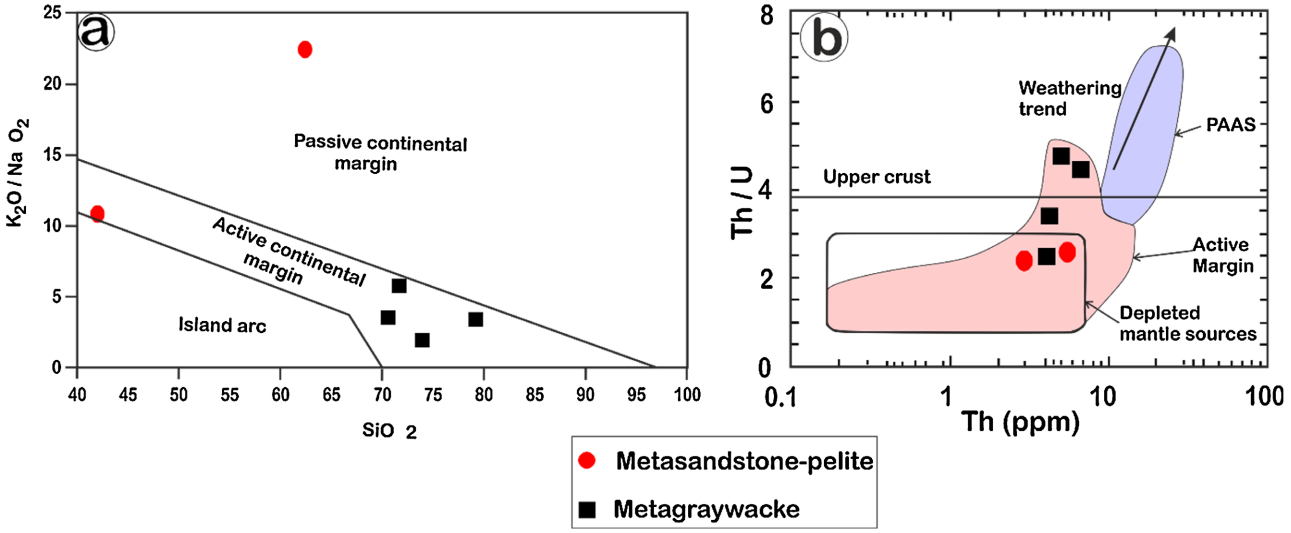

Figure 9. (a) Na_2O/K_2O versus SiO_2 diagram from Roser and Korsch (1986) applied to metasedimentary rocks of the Banfora belt. (b) Plot of Th/U versus Th for the metasedimentary rocks of the Banfora belt (after McLennan *et al.*, 1993).

that the meta-pelite sandstone and metagraywackes samples formed in an active margin context (**Figure 9(b)**). In the diagram of [55], the metapelite sandstone have a mafic to intermediate igneous origin, while the metagraywackes come from a felsic source with a mixture of a quartzite sedimentary rock source (**Figure 10**). Observation of the representative points in the ACNK diagram shows that the metapelite sandstone and metagraywackes derived from the erosion of andesite basalt and andesite-granite, respectively. Similar results have been found in the Ivory Coast in the Comoé basin [48], where the protoliths evolve between gabbros and granites, and in the SASCA domain, where the source evolves from basalts to andesites [56].

6. Conclusion

Preliminary petrographic and geochemical data show that the Banfora metasediments

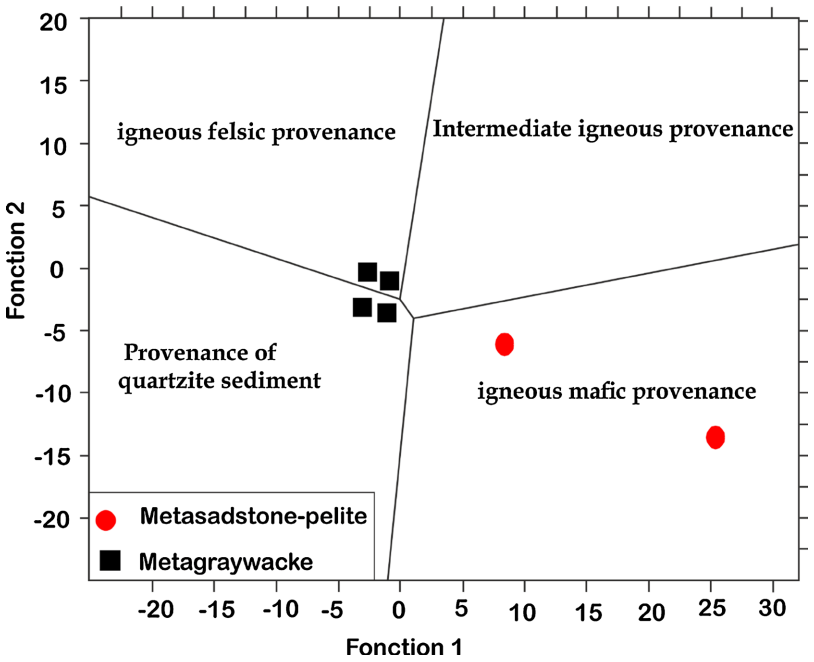

Figure 10. Discriminant function diagram Roser and Korsch (1988) applied metasedimentary rocks of the Banfora belt. Discriminant function 1: $(-1.773 * TiO_2) + (0.607 * Al_2O_3) + (0.760 * Fe_2O_3) + (-1.500 * MgO) + (0.616 * CaO) + (0.509 * Na_2O) + (-1.224 * K_2O) + (-9.090)$. Discriminant function 2: $(0.445 * TiO_2) + (0.070 * Al_2O_3) + (-0.250 * Fe_2O_3) + (-1.142 * MgO) + (0.438 * CaO) + (1.475 * Na_2O) + (-1.426 * K_2O) + (-6.861)$.

are essentially meta sandstone-pelites and metagraywackes. The meta sandstone-pelites contain a mixture of mafic and intermediate igneous sources, indicating that the protoliths could be basalts and andesites, but the metagraywackes are thought to have been derived from the erosion of a mixture of andesitic and granitic rocks. The rocks studied come from young undifferentiated to differentiated arcs. They have low sedimentary maturity and low to moderate chemical maturity. The Chemical Alteration Index (CIA) and Plagioclase Alteration Index (PIA) suggest weak to moderate alteration of the source rocks, but this is not comparable to simple alteration as the sole control on chemical composition. The samples underwent K input as a result of metasomatism.

Conflicts of Interest

The authors declare no conflicts of interest regarding the publication of this paper.

References

[1] Blatt, H. (1967) Provenance Determinations and Recycling of Sediments. *SEPM Journal of Sedimentary Research*, **37**, 1031-1044. https://doi.org/10.1306/74d71825-2b21-11d7-8648000102c1865d

[2] Dickinson, W.R. (1970) Interpreting Detrital Modes of Graywacke and Arkose. *SEPM Journal of Sedimentary Research*, **40**, 695-707. https://doi.org/10.1306/74d72018-2b21-11d7-8648000102c1865d

[3] Taylor, S.R. and McLennan, S.M. (1985) The Continental Crust: Its Composition and

Evolution. Blackwell, 312.

[4] McLennan, S.M., Hemming, S., McDaniel, D.K. and Hanson, G.N. (1993) Geochemical Approaches to Sedimentation, Provenance, and Tectonics. In: Johnsson, M.J. and Basu, A., Eds., *Geological Society of America Special Papers*, Geological Society of America, 21-40. https://doi.org/10.1130/spe284-p21

[5] Rudnick, R.L. and Gao, S. (2014) Composition of the Continental Crust. In: Holland, H. and Turekian, K., Eds., *Treatise on Geochemistry*, Elsevier, 1-51. https://doi.org/10.1016/b978-0-08-095975-7.00301-6

[6] Genna, D., Gaboury, D. and Roy, G. (2014) Evolution of a Volcanogenic Hydrothermal System Recorded by the Behavior of LREE and Eu: Case Study of the Key Tuffite at Bracemac-McLeod Deposits, Matagami, Canada. *Ore Geology Reviews*, **63**, 160-177. https://doi.org/10.1016/j.oregeorev.2014.04.019

[7] Asiedu, D.K., Asong, S., Atta-Peters, D., Sakyi, P.A., Su, B., Dampare, S.B., *et al.* (2017) Geochemical and Nd-Isotopic Compositions of Juvenile-Type Paleoproterozoic Birimian Sedimentary Rocks from Southeastern West African Craton (Ghana): Constraints on Provenance and Tectonic Setting. *Precambrian Research*, **300**, 40-52. https://doi.org/10.1016/j.precamres.2017.07.035

[8] Rudnick, R.L. and Gao, S. (2003) Composition of the Continental Crust. In: Turekian, H.D.H.K., Ed., *Treatise on Geochemistry*, Elsevier, 1-64. https://doi.org/10.1016/b0-08-043751-6/03016-4

[9] Busby, C. and Pérez, A.A. (2012) Tectonics of Sedimentary Basins Recent Advances. Wiley Blackwell, 664.

[10] Grenholm, M., Jessell, M. and Thébaud, N. (2019) Paleoproterozoic Volcano-Sedimentary Series in the Ca. 2.27 - 1.96 Ga Birimian Orogen of the Southeastern West African Craton. *Precambrian Research*, **328**, 161-192. https://doi.org/10.1016/j.precamres.2019.04.005

[11] Pouclet, A., Doumbia, S. and Vidal, M. (2006) Geodynamic Setting of the Birimian Volcanism in Central Ivory Coast (Western Africa) and Its Place in the Palaeoproterozoic Evolution of the Man Shield. *Bulletin de la Société Géologique de France*, **177**, 105-121. https://doi.org/10.2113/gssgfbull.177.2.105

[12] Lompo, M. (2009) Geodynamic Evolution of the 2.25-2.0 Ga Palaeoproterozoic Magmatic Rocks in the Man-Leo Shield of the West African Craton. A Model of Subsidence of an Oceanic Plateau. *Geological Society*, *London*, *Special Publications*, **323**, 231-254. https://doi.org/10.1144/sp323.11

[13] Baratoux, L., Metelka, V., Naba, S., Jessell, M.W., Grégoire, M. and Ganne, J. (2011) Juvenile Paleoproterozoic Crust Evolution during the Eburnean Orogeny (~2.2 - 2.0 Ga), Western Burkina Faso. *Precambrian Research*, **191**, 18-45. https://doi.org/10.1016/j.precamres.2011.08.010

[14] Ilboudo, H., Sawadogo, S., Zongo, G.H., Naba, S., Wenmenga, U. and Lompo, M. (2020) Geochemistry and Geodynamic Constraint of Volcanic and Plutonic Magmatism within the Banfora Belt (Burkina-Faso, West-Africa): Contribution to Mineral Exploration. *Geological Society*, *London*, *Special Publications*, **502**, 283-307. https://doi.org/10.1144/sp502-2019-86

[15] Mériaud, N., Thébaud, N., Masurel, Q., Hayman, P., Jessell, M., Kemp, A., *et al.* (2020) Lithostratigraphic Evolution of the Bandamian Volcanic Cycle in Central Côte d'Ivoire: Insights into the Late Eburnean Magmatic Resurgence and Its Geodynamic Implications. *Precambrian Research*, **347**, Article ID: 105847. https://doi.org/10.1016/j.precamres.2020.105847

[16] Ilboudo, H., Sawadogo, S., Kagambega, N. and Remmal, T. (2021) Petrology, Geo-

chemistry, and Source of the Emplacement Model of the Paleoproterozoic Tiébélé Granite Pluton, Burkina Faso (West-Africa): Contribution to Mineral Exploration. *International Journal of Earth Sciences*, **110**, 1753-1781. https://doi.org/10.1007/s00531-021-02039-3

[17] Hayman, P.C., Bolz, P., Senyah, G., Tegan, E., Denyszyn, S., Murphy, D.T., *et al.* (2023) Physical and Geochemical Reconstruction of a 2.35 - 2.1 Ga Volcanic Arc (Toumodi Greenstone Belt, Ivory Coast, West Africa). *Precambrian Research*, **389**, Article ID: 107029. https://doi.org/10.1016/j.precamres.2023.107029

[18] Gnamou, B., Ilboudo, H., Toé, W.A.B. and Sawadogo, S. (2023) Geochemical Mobility Associated to Gold and Base Metal Occurrences of Mangodara Sector, in Southern Burkina Faso, Banfora Greenstone Belts (West African Craton). *Open Journal of Geology*, **13**, 1024-1053. https://doi.org/10.4236/ojg.2023.1310044

[19] Gnamou, B., Ilboudo, H., Toe, W.A.B. and Sawadogo, S. (2024) Geochemical Feature of the Mangodara Metavolcanic Rocks within the Banfora Paleoproterozoic Greenstone Belts, Southern Burkina Faso (West African Craton). *Bulletin de l'Institut Scientifique, Rabat, Section Sciences de la Terre*, **46**, 31-53.

[20] Hirdes, W. and Davis, D.W. (2002) U-Pb Geochronology of Paleoproterozoic Rocks in the Southern Part of the Kedougou-Kéniéba Inlier, Senegal, West Africa: Evidence for Diachronous Accretionary Development of the Eburnean Province. *Precambrian Research*, **118**, 83-99. https://doi.org/10.1016/s0301-9268(02)00080-3

[21] Pigois, J., Groves, D.I., Fletcher, I.R., McNaughton, N.J. and Snee, L.W. (2003) Age Constraints on Tarkwaian Palaeoplacer and Lode-Gold Formation in the Tarkwa-Damang District, SW Ghana. *Mineralium Deposita*, **38**, 695-714. https://doi.org/10.1007/s00126-003-0360-5

[22] Block, S., Baratoux, L., Zeh, A., Laurent, O., Bruguier, O., Jessell, M., *et al.* (2016) Paleoproterozoic Juvenile Crust Formation and Stabilisation in the South-Eastern West African Craton (Ghana); New Insights from U-Pb-Hf Zircon Data and Geochemistry. *Precambrian Research*, **287**, 1-30. https://doi.org/10.1016/j.precamres.2016.10.011

[23] Gasquet, D., Barbey, P., Adou, M. and Paquette, J.L. (2003) Structure, Sr-Nd Isotope Geochemistry and Zircon U-Pb Geochronology of the Granitoids of the Dabakala Area (Côte d'Ivoire): Evidence for a 2.3 Ga Crustal Growth Event in the Palaeoproterozoic of West Africa? *Precambrian Research*, **127**, 329-354. https://doi.org/10.1016/s0301-9268(03)00209-2

[24] Doumbia, S., Pouclet, A., Kouamelan, A., Peucat, J.J., Vidal, M. and Delor, C. (1998) Petrogenesis of Juvenile-Type Birimian (Paleoproterozoic) Granitoids in Central Côte-D'ivoire, West Africa: Geochemistry and Geochronology. *Precambrian Research*, **87**, 33-63. https://doi.org/10.1016/s0301-9268(97)00201-5

[25] Hein, K.A.A., Matsheka, I.R., Bruguier, O., Masurel, Q., Bosch, D., Caby, R., *et al.* (2015) The Yatela Gold Deposit: 2 Billion Years in the Making. *Journal of African Earth Sciences*, **112**, 548-569. https://doi.org/10.1016/j.jafrearsci.2015.07.017

[26] Koffi, Y.H., Wenmenga, U. and Djro, S.C. (2016) Tarkwaian Deposits of the Birimian Belt of Houndé: Petrological, Structural and Geochemical Study (Burkina-Faso, West Africa). *International Journal of Geosciences*, **7**, 685-700. https://doi.org/10.4236/ijg.2016.75053

[27] Castaing, C., Billa, M., Milési, J.P., Thiéblemont, D., Le Métour, J., Egal, E., Donzeau, M., Guerrot, C., Cocherie, A., Chèvremont, P., Tegyey, M., Itard, Y., Zida, B., Ouedraogo, B., Kote, S., Kabore, B.E., Ouedraogo, C., Ki, J.C. and Zunino, C. (2003) Notice explicative de la carte géologique et minière du Burkina Faso à 1/1 000 000.

Bureau de Recherches Géologiques et Miniéres (BRGM), 148.

[28] Kouamelan, A.N., Delor, C. and Peucat, J. (1997) Geochronological Evidence for Reworking of Archean Terrains during the Early Proterozoic (2.1 Ga) in the Western Cote D'ivoire (Man Rise-West African Craton). *Precambrian Research*, **86**, 177-199. https://doi.org/10.1016/s0301-9268(97)00043-0

[29] Caby, R., Delor, C. and Agoh, O. (2000) Lithologie, structure et métamorphisme des formations birimiennes dans la région d'Odienné(Cote d'Ivoire): Role majeur du diapirisme des plutons et des décrochements en bordure du craton de Man. *Journal of African Earth Sciences*, **30**, 351-374. https://doi.org/10.1016/s0899-5362(00)00024-5

[30] Rollinson, H. (2016) Archaean Crustal Evolution in West Africa: A New Synthesis of the Archaean Geology in Sierra Leone, Liberia, Guinea and Ivory Coast. *Precambrian Research*, **281**, 1-12. https://doi.org/10.1016/j.precamres.2016.05.005

[31] Markwitz, V., Hein, K.A.A. and Miller, J. (2016) Compilation of West African Mineral Deposits: Spatial Distribution and Mineral Endowment. *Precambrian Research*, **274**, 61-81. https://doi.org/10.1016/j.precamres.2015.05.028

[32] Parra-Avila, L.A., Kemp, A.I.S., Fiorentini, M.L., Belousova, E., Baratoux, L., Block, S., *et al.* (2017) The Geochronological Evolution of the Paleoproterozoic Baoulé-Mossi Domain of the Southern West African Craton. *Precambrian Research*, **300**, 1-27. https://doi.org/10.1016/j.precamres.2017.07.036

[33] Vidal, M., Gumiaux, C., Cagnard, F., Pouclet, A., Ouattara, G. and Pichon, M. (2009) Evolution of a Paleoproterozoic "Weak Type" Orogeny in the West African Craton (Ivory Coast). *Tectonophysics*, **477**, 145-159. https://doi.org/10.1016/j.tecto.2009.02.010

[34] Lompo, M. (2010) Paleoproterozoic Structural Evolution of the Man-Leo Shield (West Africa). Key Structures for Vertical to Transcurrent Tectonics. *Journal of African Earth Sciences*, **58**, 19-36. https://doi.org/10.1016/j.jafrearsci.2010.01.005

[35] Ganne, J., De Andrade, V., Weinberg, R.F., Vidal, O., Dubacq, B., Kagambega, N., *et al.* (2011) Modern-Style Plate Subduction Preserved in the Palaeoproterozoic West African Craton. *Nature Geoscience*, **5**, 60-65. https://doi.org/10.1038/ngeo1321

[36] Augustin, J. and Gaboury, D. (2017) Paleoproterozoic Plume-Related Basaltic Rocks in the Mana Gold District in Western Burkina Faso, West Africa: Implications for Exploration and the Source of Gold in Orogenic Deposits. *Journal of African Earth Sciences*, **129**, 17-30. https://doi.org/10.1016/j.jafrearsci.2016.12.007

[37] Bonzi, W.M., Vanderhaeghe, O., Van Lichtervelde, M., Wenmenga, U., André-Mayer, A., Salvi, S., *et al.* (2021) Petrogenetic Links between Rare Metal-Bearing Pegmatites and TTG Gneisses in the West African Craton: The Mangodara District of SW Burkina Faso. *Precambrian Research*, **364**, Article ID: 106359. https://doi.org/10.1016/j.precamres.2021.106359

[38] Milési, J.P., Feybesse, J.L., Ledru, P., Dommanget, A., Ouédraogo, M.F., Marcoux, E., Prost, A.E., Vinchon, C., Sylvain, J.P., Johan, V., Teguey, M., Calvez, J.Y. and La-gny, P. (1989) Les minéralisations aurifères d'Afrique de l'Ouest. Leurs relations avec l'évolution lithostructurale au Protérozoïque inférieur. *Chroniques Recherche Minière France*, **497**, 3-98.

[39] Ilboudo, H., Wenmenga, U. and Sawadogo, S. (2017) Mise en évidence d'un assemblage à disthène-staurotide—Grenat dans le secteur de Mangodara, ceinture de Banfora, Burkina Faso, Afrique de l' Ouest: Implication dans la genèse des gîtes minéraux polymétalliques. *Afrique Science*, **13**, 220-223.

[40] Parra-Avila, L.A., Baratoux, L., Eglinger, A., Fiorentini, M.L. and Block, S. (2019) The Eburnean Magmatic Evolution across the Baoulé-Mossi Domain: Geodynamic Im-

plications for the West African Craton. *Precambrian Research*, **332**, Article ID: 105392. https://doi.org/10.1016/j.precamres.2019.105392

[41] Ouattara, G. (1998) Structure du Batholite de Ferkessédougou (Secteur de Zuenoula, Côte d'Ivoire). Master's Thesis, Université d'Orléans.

[42] Bonzi, W.M., Van Lichtervelde, M., Vanderhaeghe, O., André-Mayer, A., Salvi, S. and Wenmenga, U. (2022) Insights from Mineral Trace Chemistry on the Origin of NYF and Mixed LCT + NYF Pegmatites and Their Mineralization at Mangodara, SW Burkina Faso. *Mineralium Deposita*, **58**, 75-104. https://doi.org/10.1007/s00126-022-01127-x

[43] Kretz, R. (1983) Symbols for Rock-Forming Minerals. *American Mineralogist*, **68**, 277-279.

[44] Herron, M.M. (1988) Geochemical Classification of Terrigenous Sands and Shales from Core or Log Data. *SEPM Journal of Sedimentary Research*, **58**, 820-829. https://doi.org/10.1306/212f8e77-2b24-11d7-8648000102c1865d

[45] Roddaz, M., Debat, P. and Nikiema, S. (2007) Geochemistry of Upper Birimian Sediments (Major and Trace Elements and Nd-Sr Isotopes) and Implications for Weathering and Tectonic Setting of the Late Paleoproterozoic Crust. *Precambrian Research*, **159**, 197-211. https://doi.org/10.1016/j.precamres.2007.06.008

[46] Tshibubudze, A., Hein, K.A.A., Peters, L.F.H., Woolfe, A.J. and McCuaig, T.C. (2013) Oldest U-Pb Crystallisation Age for the West African Craton from the Oudalan-Gorouol Belt of Burkina Faso. *South African Journal of Geology*, **116**, 169-181. https://doi.org/10.2113/gssajg.116.1.169

[47] Asiedu, D.K., Agoe, M., Amponsah, P.O., Nude, P.M. and Anani, C.Y. (2019) Geochemical Constraints on Provenance and Source Area Weathering of Metasedimentary Rocks from the Paleoproterozoic (~2.1 Ga) Wa-Lawra Belt, Southeastern Margin of the West African Craton. *Geodinamica Acta*, **31**, 27-39. https://doi.org/10.1080/09853111.2019.1670414

[48] Adingra, M.P.K., Coulibaly, Y., Ouattara, Z. and Coulibaly, I. (2018) Caractéristiques pétrographiques et géochimiques des métasédiments de la partie sud-est du bassin de la Comoé (Nord d'Alépé, sudest de la Côte d'Ivoire). *Revue RAMReS, Sciences de la vie, de la terre et agronomie*, **6**, 28-35.

[49] Teha, K.R., Pria, K.K.J., Koffi, A.Y., Brou, K.J., Kouassi, B.R. and Kouamelan, A.N. (2023) Tracing the Sources of Paleoproterozoic Metasediments in the Comoé Basin, Côte D'ivoire, West Africa: Geochemistry Implication. *Journal of Geography, Environment and Earth Science International*, **27**, 113-129. https://doi.org/10.9734/jgeesi/2023/v27i10720

[50] Leube, A., Hirdes, W., Mauer, R. and Kesse, G.O. (1990) The Early Proterozoic Birimian Supergroup of Ghana and Some Aspects of Its Associated Gold Mineralization. *Precambrian Research*, **46**, 139-165. https://doi.org/10.1016/0301-9268(90)90070-7

[51] Bossière, G., Bonkoungou, I., Peucat, J. and Pupin, J. (1996) Origin and Age of Paleoproterozoic Conglomerates and Sandstones of the Tarkwaian Group in Burkina Faso, West Africa. *Precambrian Research*, **80**, 153-172. https://doi.org/10.1016/s0301-9268(96)00014-9

[52] Lebrun, E., Miller, J., Thébaud, N., Ulrich, S. and McCuaig, T.C. (2017) Structural Controls on an Orogenic Gold System: The World-Class Siguiri Gold District, Siguiri Basin, Guinea, West Africa. *Economic Geology*, **112**, 73-98. https://doi.org/10.2113/econgeo.112.1.73

[53] Rollinson, H.R. (1993) Using Geochemical Data Evaluation, Presentation, Interpre-

tation. John Wiley & Sons, 352.

[54] Land, L.S. (1984) Frio Sandstone diagenesis, Texas Gulf Coast: A Regional Isotopic Study. In: McDonald, D.A. and Surdam, R.C., Eds., *Clastic Genesis*, American Association of Petroleum Geologists Memoir, 47-62.

[55] Roser, B.P. and Korsch, R.J. (1986) Determination of Tectonic Setting of Sandstone-Mudstone Suites Using SiO_2 Content and K_2O/Na_2O Ratio. *The Journal of Geology*, **94**, 635-650. https://doi.org/10.1086/629071

[56] Koffi, Y.A., Kouamelan, A.N., Kouadio, F.J.L.H., Teha, K.R., Kouassi, B.R. and Koffi, G.R.S. (2018) Pétrographie et origine des métasédiments du domaine SASCA (SW de la Côte d'Ivoire). *International Journal of Innovation and Applied Studies*, **23**, 451-464.